Influence of Obstacles on the Mixing Performance of Serpentine Microchannels

Kailas Malgonde, Babruvahan P. Ronge, and Sandeep S. Wangikar

Abstract The several Lab on a Chip devices depend largely on the microchannels. Each microchannel's performance is determined by its mixing properties and pressure drop. The performance evaluation for serpentine microchannels including obstacles is the main topic of this paper. The simulations based on computational fluid dynamics (CFD) were performed by employing COMSOL Multiphysics 5.0 software. The semicircular obstacles were introduced in the flow direction of serpentine microchannels. The two inlets' entrance velocities ranged between 0.5, 0.75 and 1 mm/s. The microchannels' width and height were 400 μm (for an aspect ratio of 1). Pressure changes (drops) and mixing in straight serpentine microchannels with no obstructions and semi-circular obstructions are discussed. Study is done on how inlet velocity affects pressure drop as well as mixing length.

Keywords Serpentine microchannel · Semicircular obstacles · Curved bend · Mixing length · Pressure drop

1 Introduction

Microfluidics is a concept that describes fluid control and actuation methods and components used for microscopic level fluid transport phenomena. The field of microfluidic systems is one that is rapidly developing, and research in this area is crucial to the implementation of lab-on-a chip (LOC). The LOC systems, also known as systems for micro total analysis (μTAS), are capable of carrying out the full range of biological and chemical processes [1, 2]. Numerous industries, such as cosmetics, medicine, pharmaceuticals, and biotechnology as well as the control systems using physical sciences and heat management, use microfluidics. One of the essential parts of microfluidic systems is a microchannel. The term "microchannel" refers to a channel with dimensions in the micrometer (μm) range. A micromixer is

K. Malgonde (✉) · B. P. Ronge · S. S. Wangikar
Department of Mechanical Engineering, SVERI's College of Engineering, Pandharpur, Maharashtra, India
e-mail: kailas_mallu@yahoo.com

a microchannel only which is employed for mixing fluids. The microfluidic chips, which are circuits, already have the geometries in place. Since this technology provides a way to perform the crucial chemical evaluation processes in the biomedical field, it has been the subject of extensive research [1–3]. Micromixers can always be split into 2 groups: passive and active. These micromixers differ in terms of capacity, mixing speed, and operational needs. For instance, a power source is needed to enable mixing in an active micromixer.

A passive micromixer, in contrast, uses applied pressure meant for fluid motion to achieve mixing. As a result, several micromixers better suited than others for a given application. Although integration with other devices is challenging and fabrication is expensive, active micromixers typically offer accurate mixing. Because of this, passive micromixers are frequently preferred [4–6].

Numerous studies discuss the mixing capabilities of passive microchannels. Different researchers have used a variety of geometries, including wavy structures, curved shapes, static micromixers, square waves, straight microchannels, spiral-shaped microchannels, serpentine microchannels with non-aligned inputs, serpentine microchannels with cyclic L-shaped units, etc. to investigate impact of geometry along with profile on mixing performance [7–15]. The split-and-recombine (SAR) microchannel has also been a subject of extensive research. To improve the diffusion process, SAR splits and recombines the two fluids that need to be mixed. Planar SAR micromixers, P-SAR micromixers with cavities, modified P-SAR micromixers with dislocation sub-channels, two-layer crossing channels, 2D modified Tesla structures, ellipse-like micropillars, etc. are a few examples of the various configurations of passive micromixers created by a number of researchers. The split and recombining mechanism and the resulting chaotic advection have been observed to improve mixing performance [16–18]. Lots of studies using various varieties of grooves and obstacles across the mixing path to study the mixing behavior of microchannels have been published by different researchers. [19–24] and reported that performance of mixing was improved on account of the creation of recirculation zones downstream of these obstructions. A select group of researchers have created microchannels using a variety of techniques, including micro-milling, laser machining, and photochemical machining [25–35].

Based on the aforementioned studies, it can be deduced that the mixing index (also known as mixing length) and pressure drop are the two main factors that control the behavior of the microchannel. However, a comparison of microchannels that are serpentine and have both straight and curved bends is still possible. Also impressive is how width as well as height (i.e. aspect ratio) affects the analysis of mixing. The mixing performance analysis for microchannels with obstacles is presented in this paper. These simulations were done with the aid of COMSOL Multiphysics 5.0. Analysis is done on pressure change (drop) and combining in serpentine microchannels with and without semicircular obstructions.

Fig. 1 Serpentine microchannel **a** without obstruction **b** including semi-circular obstruction

(a) (b)
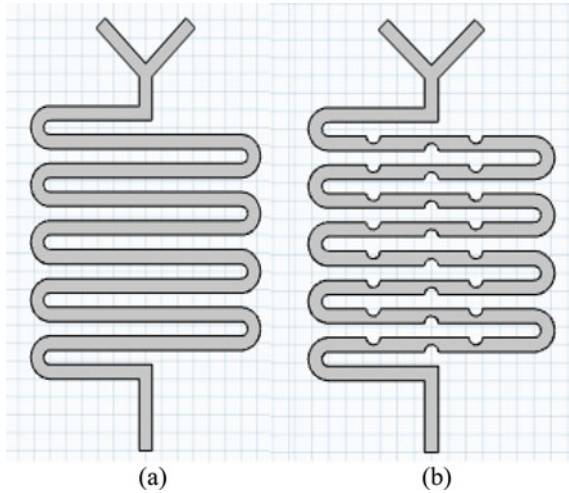
2 Numerical Simulations as a Methodology

2.1 Microchannel Configuration

Inside this current study, a serpentine microchannel with no obstacles and a serpentine microchannel using semicircular obstacles have both been taken into consideration. COMSOL Multiphysics 5.0 was used to create the computational models, which are shown in Fig. 1a, b for serpentine microchannel with as well as without semicircular obstacles, in that order. In each configurations of aspect ratio 1, microchannel's sizes (width and height) are 400 m. Semicircular obstacles have a 200 m radius. Inlet 1 and Inlet 2 were used for feeding the two fluids. For both inlets, it has been assumed that the velocity of fluid (u mm/s) is the same.

2.2 Boundary Criteria

COMSOL Multiphysics 5.0 has been used to run the various simulations for the created microchannels. Laminar flow and the transportation of diluted species are the physics used during COMSOL simulations. Governing equations or Eqs. 1–3, were solved by the software using appropriate boundary conditions. The used boundary conditions include no-slip conditions at the microchannel walls, equal velocities at the both the inlets, atmospheric pressure at the outlet, symmetry at the fluid-to-fluid interface, and equal velocities at the two inlets. Water and ethanol at a temperature of 25 °C have been assumed to be the fluids at the two inlets. The fluid concentrations

just at inlet boundaries have been calculated as 10 mol/m^3 for fluids and 0 mol/m^3 for fluid 2. It has been determined that ethanol's water diffusion coefficient is 1.0×10^{-9} m^2/s Inlet velocity is adjusted between 0.5 and 1 mm/s.

The steady state conditions used for fluid flow, as well as convection and species diffusion, have been considered for the established computational models. The Navier-Stokes as well as continuity equations are used to express the incompressible isothermal Newtonian fluids in microchannels' mass-momentum balance. These are the equations:

$$\nabla.u = 0 \tag{1}$$

$$\rho(u.\nabla)u = \nabla.[-pI + \mu(\nabla u + (\nabla u)^{T}) - 2/3\mu(\nabla.u)I] + F \tag{2}$$

where I is unit diagonal matrix, u $=$ (u, v, w) is flow velocity field, μ is the fluid dynamic viscosity, p is fluid pressure, ρ is density of fluid, and F $=$ (fx, fy, fz) is a fluid-affecting volume force.

Diffusion and convection cause the fluid flow to mix as a result. Mass transportation has been governed by the formula:

$$\nabla.(-D.\nabla c) + u.\nabla c = R \tag{3}$$

2.3 Mesh Generation

Unstructured mesh was used for the computational analysis (CFD) of micro channel models. The simulations were run with various mesh sizes (domain elements) to prevent the impact of more meshing elements on the simulation results' quality. The pressure drop results at various domain elements are compared for both microchannel configurations. Figure 2a as well as b show the mesh-enclosed serpentine microchannel with parallel oblique bends, respectively.

3 The Study Results and Discussion

The COMSOL Multiphysics 5.0 tool was used to create the serpentine microchannel's three-dimensional models, which include both straight and curved bends, and then run simulations on them. By taking into account the conditions of the boundary, Eqs. 1 through 3 have been solved. The primary fluid is water, and the secondary fluid is ethanol, both at a temperature of 25 °C.
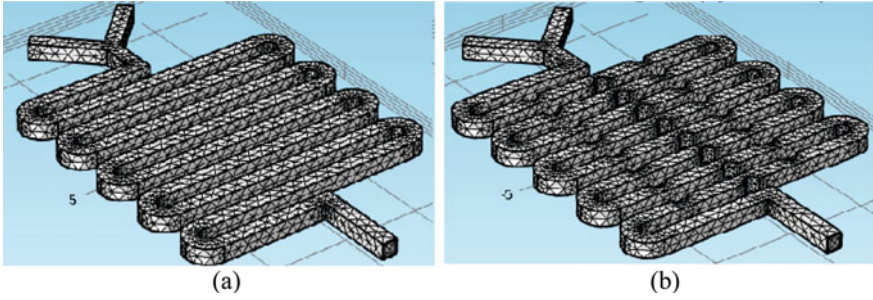
Fig. 2 Serpentine microchannel meshing **a** with no obstacles **b** with semicircular obstacles

3.1 Impact (in Pa) on the Drop in Pressure

Analysis is done on how the aspect ratio affects the pressure drop. There were three different inlet fluid velocities tested: 0.5, and 0.75, and 1 mm/s. Figure 3a, b respectively show the sample pictures for the pressure drop measurement for the Serpentine microchannel (a) without obstacles and (b) with semicircular obstacles.

The pressure drop was measured, and Fig. 4 illustrates how the aspect ratio affected the pressure drop for serpentine microchannels with and without semicircular obstacles. Figure 4 shows that the pressure drop increases as the velocity rises from 0.5 to 1 mm/s. The pressure drop for serpentine micro channels with semicircular obstacles is higher than it is for channels without obstacles, it is also noted. This is due to the fact that the cross-sectional area of the microchannel grows as the aspect ratio does. The pressure on a fluid will be greater in a smaller area and lower in a larger area. Due to the shape of the obstacles, the fluids are subjected to greater pressure there, which causes a greater pressure drop in a serpentine microchannel with semicircular obstacles.
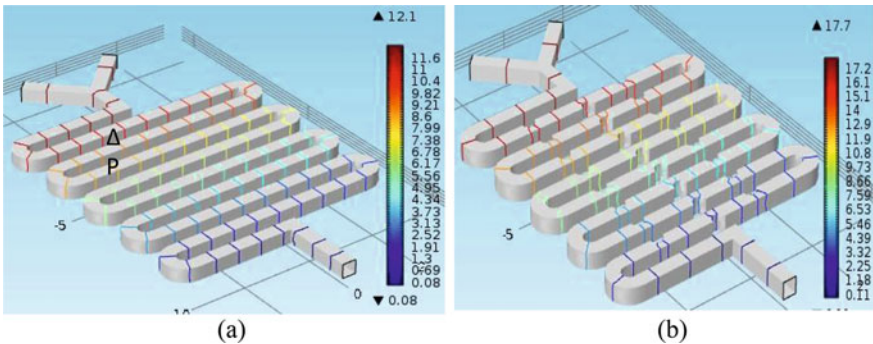

Fig. 3 Pressure drop for **a** serpentine microchannel with no obstacles **b** serpentine microchannel with semicircular obstacles
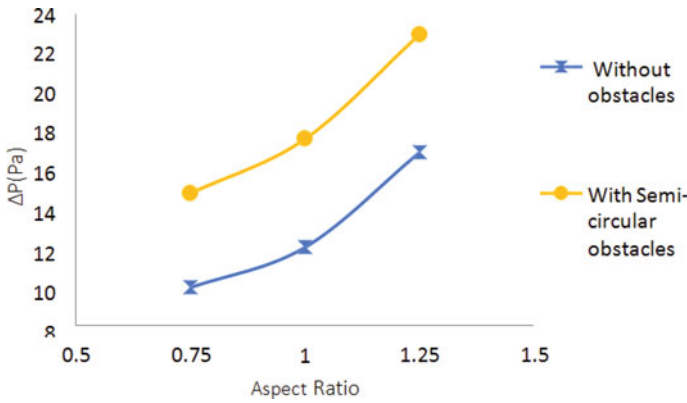
Fig. 4 Relationship between aspect ration and pressure drop

3.2 Impact on Mixing Length

The phrase "mixing length" refers to the length of the channel at which the two fluids are completely mixed, or when the mixing index is 1. In the COMSOL Multiphysics 5 program, the mixing duration is recorded. Figure 5 shows examples of the cross-sectional mixture images for a Serpentine microchannel (a) with no obstacles and (b) with semicircular obstacles.

Figure 6 shows that the mixing length is significantly shorter for microchannels with semicircular obstacles than it is for channels without obstacles. This increase results from the fact that the flow is laminar at lower fluid velocities and that diffusion causes mixing in the microchannels. This shorter mixing length results from chaotic advection and vortices that form near semicircular obstacles, which improve mixing and result in shorter mixing lengths than for situations without obstacles.
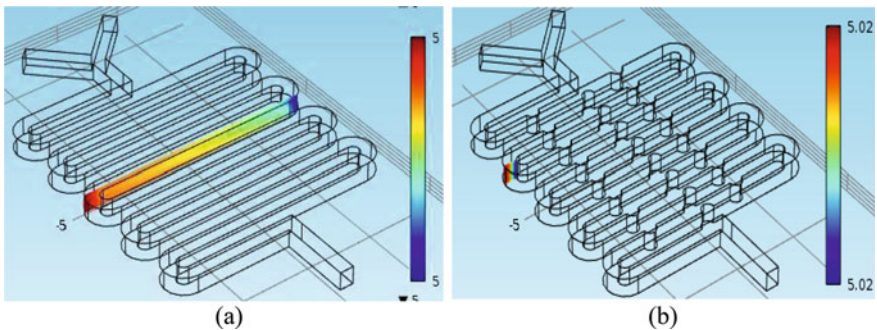

Fig. 5 Few images of mixing at the channel's cross-section for a serpentine microchannel **a** without obstacles **b** with semicircular obstacles
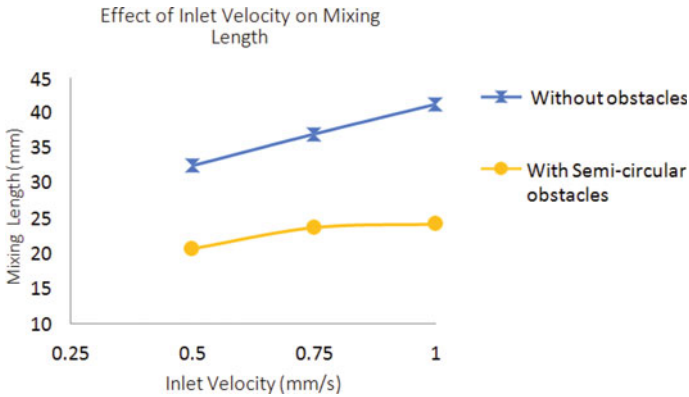
Fig. 6 Mixing length for Serpentine microchannel **a** with no obstacles **b** with semicircular obstacles

4 Conclusions

Using computational analysis by means of COMSOL Multiphysics 5.0 tool, the mixing performance analysis of a Serpentine microchannel (a) without obstacles and (b) with semicircular obstacles has been studied. Investigation is done into how inlet velocity affects the pressure drop as well as mixing length. The following conclusions have been drawn from the numerical analysis:

- As inlet velocity increases, the pressure drop also grows.
- In comparison to serpentine microchannels without obstacles, higher pressure drops are observed in serpentine microchannels with semicircular obstacles.
- In comparison to serpentine microchannels without obstacles, shorter mixing lengths are observed for semicircular obstacles.

References

1. Lee, C. Y., Wang, W. T., Liu, C. C., & Fu, L. M. (2016). Passive mixers in microfluidic systems: A review. *Chemical Engineering Journal, 288*, 146–160.
2. Lim, Y. C., Kouzani, A. Z., & Duan, W. (2010). Lab-on-a-chip: A component view. *Microsystem Technologies, 16*(12), 1995–2015.
3. Whitesides, G. M. (2006). The origins and the future of microfluidics. *Nature, 442*(7101), 368–373.
4. Bothe, D., Stemich, C., & Warnecke, H. J. (2006). Fluid mixing in a T-shaped micro-mixer. *Chemical Engineering Science, 61*(9), 2950–2958.
5. Bahrami, M., Yovanovich, M. M., & Culham, J. R. (2005). Pressure drop of fully-developed, laminar flow in microchannels of arbitrary cross-section. *International Conference on Nanochannels, Microchannels, and Minichannels, 41855*, 269–280.

6. Song, H., Wang, Y., & Pant, K. (2012). Cross-stream diffusion under pressure-driven flow in microchannels with arbitrary aspect ratios: A phase diagram study using a three-dimensional analytical model. *Microfluidics and Nanofluidics, 12*(1–4), 265–267.

7. Ansari, M. A., Kim, K. Y., & Kim, S. M. (2010). Numerical study of the effect on mixing of the position of fluid stream interfaces in a rectangular microchannel. *Microsystem Technologies, 16*(10), 1757–1763.

8. Gobby, D., Angeli, P., & Gavriilidis, A. (2001). Mixing characteristics of T-type microfluidic mixers. *Journal of Micromechanics and Microengineering, 11*(2), 126.

9. Cortes-Quiroz, C. A., Azarbadegan, A., & Zangeneh, M. (2014). Evaluation of flow characteristics that give higher mixing performance in the 3-D T-mixer versus the typical T-mixer. *Sensors and Actuators B: Chemical, 31*(202), 1209–1219.

10. Lü, Y., Zhu, S., Wang, K., & Luo, G. (2016). Simulation of the mixing process in a straight tube with sudden changed cross-section. *Chinese Journal of Chemical Engineering, 24*(6), 711–718.

11. Yang, I. D., Chen, Y. F., Tseng, F. G., Hsu, H. T., & Chieng, C. C. (2006). Surface tension driven and 3-D vortex enhanced rapid mixing microchamber. *Journal of Microelectromechanical Systems, 15*(3), 659–670.

12. Sudarsan, A. P., & Ugaz, V. M. (2006). Fluid mixing in planar spiral microchannels. *Lab on a Chip, 6*(1), 74–82.

13. Hossain, S., & Kim, K. Y. (2015). Mixing performance of a serpentine micromixer with non-aligned inputs. *Micromachines, 6*(7), 842–854.

14. Gidde, R. R., Pawar, P. M., Ronge, B. P., Shinde, A. B., Misal, N. D., & Wangikar, S. S. (2019). Flow field analysis of a passive wavy micromixer with CSAR and ESAR elements. *Microsystem Technologies, 25*(3), 1017–1030.

15. Das, S. S., Tilekar, S. D., Wangikar, S. S., & Patowari, P. K. (2017). Numerical and experimental study of passive fluids mixing in micro-channels of different configurations. *Microsystem Technologies, 23*(12), 5977–5988.

16. Hong, C. C., Choi, J. W., & Ahn, C. H. (2004). A novel in-plane passive microfluidic mixer with modified Tesla structures. *Lab on a Chip, 4*(2), 109–113.

17. Xia, G., Li, J., Tian, X., & Zhou, M. (2012). Analysis of flow and mixing characteristics of planar asymmetric split-and-recombine (P-SAR) micromixers with fan-shaped cavities. *Industrial & Engineering Chemistry Research, 51*(22), 7816–7827.

18. Li, J., Xia, G., & Li, Y. (2013). Numerical and experimental analyses of planar asymmetric split-and-recombine micromixer with dislocation sub-channels. *Journal of Chemical Technology & Biotechnology, 88*(9), 1757.

19. Tran-Minh, N., Dong, T., & Karlsen, F. (2014). An efficient passive planar micromixer with ellipse-like micropillars for continuous mixing of human blood. *Computer Methods and Programs in Biomedicine, 117*(1), 20–29.

20. Guo, L., Xu, H., & Gong, L. (2015). Influence of wall roughness models on fluid flow and heat transfer in microchannels. *Applied Thermal Engineering, 84*, 399–408.

21. Jain, M., Rao, A., & Nandakumar, K. (2013). Numerical study on shape optimization of groove micromixers. *Microfluidics and Nanofluidics, 15*(5), 689–699.

22. Kim, D. S., Lee, S. W., Kwon, T. H., & Lee, S. S. (2004). A barrier embedded chaotic micromixer. *Journal of Micromechanics and Microengineering, 14*(6), 798.

23. Wangikar, S. S., Patowari, P. K., & Misra, R. D. (2018). Numerical and experimental investigations on the performance of a serpentine microchannel with semicircular obstacles. *Microsystem Technologies, 24*(8), 3307–3320.

24. Jadhav, S. V., Pawar, P. M., Wangikar, S. S., Bhostekar, N. N., & Pawar, S. T. (2020). Thermal management materials for advanced heat sinks used in modern microelectronics. In *IOP Conference Series: Materials Science and Engineering* (Vol. 814, No. 1, p. 012044). IOP Publishing.

25. Wangikar, S. S., Patowari, P. K., & Misra, R. D. (2017). Effect of process parameters and optimization for photochemical machining of brass and German silver. *Materials and Manufacturing Processes, 32*(15), 1747–1755.

26. Wangikar, S. S., Patowari, P. K., & Misra, R. D. (2016). Parametric optimization for photochemical machining of copper using grey relational method. In *Techno-Societal 2016, International Conference on Advanced Technologies for Societal Applications* (pp. 933–943). Springer.

27. Wangikar, S. S., Patowari, P. K., & Misra, R. D. (2018). Parametric optimization for photochemical machining of copper using overall evaluation criteria. *Materials Today: Proceedings, 5*(2), 4736–4742.

28. Wangikar, S. S., Patowari, P. K., Misra, R. D., & Misal, N. D. (2019). Photochemical machining: a less explored non-conventional machining process. In *Non-conventional machining in modern manufacturing systems* (pp. 188–201). IGI Global.

29. Chavan, N. V., Bhagwat, R. M., Gaikwad, S. S., Shete, S. S., Kashid, D. T., & Wangikar S. S. (2019). Fabrication & characterization of microfeatures on PMMA using CO_2 laser machining. *International Journal for Trends in Engineering and Technology, l36*, 29–32.

30. Kulkarni, H. D., Rasal, A. B., Bidkar, O. H., Mali, V. H., Atkale, S. A., Wangikar, S. S., & Shinde, A. B. (2019). Fabrication of micro-textures on conical shape hydrodynamic journal bearing. *International Journal for Trends in Engineering and Technology, 36*(1), 37–41.

31. Raut, M. A., Kale, S. S., Pangavkar, P. V., Shinde, S. J., Wangikar, S. S., Jadhav, S. V., & Kashid, D. T. (2019). Fabrication of micro channel heat sink by using photo chemical machining. *International Journal of New Technology and Research, 5*(4), 72–75.

32. Jadhav, S.V., Pawar, P. M., Shinde, A. B., & Wangikar, S. S. (2018). Performance analysis of elliptical pin fins in the microchannels. In *Techno-Societal 2018* (pp. 295–304). Springer.

33. Bhagwat, R. M., Gaikwad, S. S., Shete, S. S., Chavan, N. V., & Wangikar, S. S. (2020). Study of etchant concentration effect on the edge deviation for photochemical machining of copper. *Novyi MIR Research Journal, 5*(9), 38–44.

34. Patil, P. K., Kulkarni, A. M., Bansode, A. A., Patil, M. K., Mulani, A. A., & Wangikar, S. S. (2020). Fabrication of logos on copper material employing photochemical machining. *Novyi MIR Research Journal, 5*(7), 70–73.

35. Kame, M. M., Sarvagod, M. V., Namde, P. A., Makar, S. C., Jadhav, S. V., & Wangikar, S. S. (2020). Fabrication of microchannels having different obstacles using photo chemical machining process *Novyi MIR Research Journal, 5*(6), 27–32.